September 2026
Volume 2
Issue 4

DOI: 10.48308/ijce.2026.247804.1039

Interdisciplinary Journal of Civil Engineering
Shahid Beheshti University

Mechanical Performance and Water Absorption Behavior of Eco-friendly Concrete Reinforced with Steel Fibers (SFs) and Waste Ceramic Powder (WCP): Experimental Study and Non-Linear Regression Modeling

Authors:

Babak Behforouz[1,*], Hamed Barghikar[2] , Sajad Fereydoonpour[3] , Mohammad Bagheri Khoulenjani[1]

Abstract

The growing demand for sustainable construction materials has encouraged the incorporation of industrial wastes into cement-based composites. This study investigates the combined effects of waste ceramic powder (WCP) as a partial cement replacement and steel fibers (SFs) as discrete reinforcement on concrete's mechanical and durability-related properties. Fifteen mixtures were prepared with WCP replacement levels of 0, 10, 20, 30, and 40% and SF volume fractions of 0, 0.75, and 1.5%. Compressive strength was measured at 7, 14, 28, and 90 days, while splitting tensile strength, flexural strength, and water absorption were evaluated at 90 days. Moderate WCP replacement improved long-term strength development through filler effects and possible pozzolanic activity, with optimum compressive performance at approximately 10% WCP. Higher replacement levels reduced strength because of cement dilution. SFs significantly enhanced tensile and flexural performance through crack bridging, while their influence on compressive strength remained limited. Combining WCP and SFs produced beneficial effects, particularly at moderate replacement levels and higher fiber dosages. Cubic regression models and response surface analysis were employed to predict concrete properties and evaluate variable interactions. High coefficients of determination

1. Water Studies Research Center, Isf.C., Islamic Azad University, Isfahan, Iran

2. Department of Mechanical Engineering, Technical and Vocational University (TVU), Tehran, Iran

3. Faculty of Engineering, Danesh Pajouhan Pishro Institute of Higher Education, Isfahan, Iran

*Corresponding Author: babakbehforouz@iau.ac.ir

Copyright: © 2026 by the authors. Submitted for possible open access publication under the terms and conditions of the Creative Commons Attribution (CC BY 4.0) International License (https://creativecommons.org/licenses/by/4.0/).

indicated good model fit. Overall, WCP–SF concrete represents a promising eco-efficient material for sustainable construction applications.

Keywords: Waste Ceramic Powder, Steel Fibers, Sustainable Concrete, Mechanical Properties, Water Absorption, Cubic Regression Modeling

1. Introduction

The rapid expansion of global infrastructure and urbanization has substantially increased the demand for concrete, making it the most widely consumed manufactured construction material worldwide. However, Portland cement production is an energy-intensive process responsible for approximately 5–8% of global anthropogenic CO_2 emissions (Mahasenan et al., 2003). Meanwhile, the ceramic manufacturing industry generates substantial quantities of non-biodegradable waste, posing significant environmental challenges associated with landfill disposal and inefficient resource utilization. Consequently, incorporating waste ceramic powder (WCP) as a supplementary cementitious material (SCM) represents a promising strategy for reducing cement consumption, mitigating environmental impacts, and promoting circular economy principles (Pacheco-Torgal & Jalali, 2010). Nevertheless, conventional concrete remains inherently brittle, with limited tensile strength and poor post-cracking behavior. The simultaneous incorporation of WCP and steel fibers (SFs) may therefore provide a complementary approach to improving mechanical performance while reducing dependence on Portland cement (Behbahani et al., 2011).

Early investigations by Song and Hwang (2004) demonstrated the effectiveness of steel fiber-reinforced concrete (SFRC), reporting that incorporating SFs at volume fractions of up to 2% increased tensile and flexural strengths by 98.3% and 126.6%, respectively, through enhanced crack-bridging mechanisms (Song & Hwang, 2004). Lopez et al. (2007) investigated ceramic waste as a partial replacement for fine aggregates, demonstrating that replacement levels of up to 50% could improve compressive strength through enhanced mechanical interlocking (Lopez et al., 2007). Similarly, Thomas and Ramaswamy (2007) reported that incorporating 1.5% SFs increased tensile and flexural capacities by approximately 40% and developed empirical relationships accounting for fiber–matrix interactions (Thomas & Ramaswamy, 2007). Subsequently, Bhargava and Banthia (2008) demonstrated that cellulose fiber reinforcement reduced water permeability and predicted chloride diffusion coefficients by up to 75%, highlighting the importance of fiber-mediated crack control in governing transport-related properties and service-life performance (Bhargava & Banthia, 2008).

Heidari and Tavakoli (2013) investigated the individual and combined effects of WCP and nano-silica (NS) on concrete performance. Although increasing WCP content generally

reduced early-age compressive strength, replacement levels of up to 20% resulted in relatively minor long-term strength reductions. Furthermore, incorporating 20% WCP reduced water absorption by 13.53%, while the combination of 10% WCP and 1% NS achieved a 91-day compressive strength of 47.8 MPa. These findings demonstrated the potential of complementary additives to compensate for the mechanical limitations of WCP-modified concrete (Heidari & Tavakoli, 2013).

Kannan et al. (2017) investigated high-strength concrete incorporating 10–40% WCP, reporting improved slump retention and reductions in chloride permeability of up to 90%, primarily attributed to particle packing and microstructural densification (Kannan et al., 2017). Subaşı et al. (2017) identified approximately 15% WCP as a favorable replacement level for balancing rheological and mechanical properties in self-compacting concrete (Subaşı et al., 2017). Extending these investigations to elevated-temperature conditions, Mohit and Sharifi (2019) demonstrated that incorporating 20–25% WCP could mitigate thermal degradation and microcracking in cement mortars exposed to temperatures of up to 800 °C. Collectively, these studies highlighted the potential physical and chemical contributions of ceramic waste to cementitious systems (Mohit & Sharifi, 2019).

In 2020, AlArab et al. investigated the potential of ceramic waste as a value-added pozzolanic material, emphasizing its complementary interactions with blast furnace slag in blended cementitious systems (AlArab et al., 2020). Behforouz et al. (2020) employed regression and artificial neural network (ANN) models to predict the performance of concrete incorporating 5–50% WCP, identifying approximately 20% replacement as favorable for maintaining compressive strength and improving electrical resistivity (Behforouz et al., 2020). Subsequently, Gautam et al. (2021) reviewed the utilization of ceramic waste in construction materials, identifying replacement levels of 10–30% as generally promising for achieving satisfactory mechanical and durability-related performance (Gautam et al., 2021). However, the variability of reported findings indicated that the effectiveness of WCP strongly depends on its physicochemical characteristics, processing conditions, and mixture composition.

Ghonaim and Morsy (2023) investigated ceramic fine dust (CFD) as a supplementary cementitious material at replacement levels ranging from 0 to 30%. Incorporating 10% CFD increased the 28-day compressive strength from 40 to 45 MPa and reduced water absorption by approximately 15%, whereas 7% CFD enhanced flexural and splitting tensile strengths by approximately 8% and 5%, respectively. Microstructural observations revealed improved matrix compactness at moderate replacement levels. Nevertheless, higher CFD contents adversely affected workability and mechanical performance, while sulfuric acid exposure resulted in strength degradation, emphasizing the importance of replacement-level optimization (Ghonaim & Morsy, 2023).

More comprehensive investigations were conducted in 2024. Li et al. (2024) reported that incorporating 10% WCP enhanced the 28-day compressive strength, whereas 20% replacement

resulted in a 10.3% reduction. Although WCP improved thermal insulation characteristics, its incorporation reduced workability and increased water absorption by up to 8.3%. These findings contrasted with previously reported reductions in water absorption, indicating that ceramic waste incorporation does not necessarily guarantee improved transport-related performance (Li et al., 2024).

Tawfik et al. (2024) investigated the individual and combined effects of WCP and waste brick powder (WBP) in high-strength concrete. Although their individual incorporation generally reduced mechanical performance, combining 5% WBP with 10% WCP improved mechanical properties and microstructural compactness compared with mixtures containing WCP alone. Furthermore, replacing 15% of cement with either material reduced specific energy consumption by 13.1% (Tawfik et al., 2024). Taher et al. (2024) subsequently demonstrated that thermal activation of WCP at 700 °C increased its 28-day strength activity index from 67.2% to 95.3%. Concrete incorporating 10% thermally treated WCP exhibited mechanical properties approaching those of conventional concrete, highlighting the importance of material processing and pozzolanic reactivity (Taher et al., 2023).

Recent investigations in 2025 increasingly emphasized computational modeling and advanced material characterization. Özkılıç et al. (2025) investigated concrete incorporating 10–50% WCP, reporting reductions in compressive, splitting tensile, and flexural strengths ranging from 5.8–73.6%, 6.3–65.4%, and 15.3–54.1%, respectively. These reductions were attributed primarily to cement dilution and inadequate particle–matrix bonding. Nevertheless, the developed ANN models achieved cross-validated coefficients of determination (R^2) of 0.945, 0.901, and 0.856 for the respective mechanical properties, demonstrating the potential of data-driven performance prediction (Özkılıç et al., 2025).

Similarly, Nasr et al. (2025) employed advanced machine learning techniques to characterize the performance of WCP-based sustainable concrete, further demonstrating the applicability of computational approaches to nonlinear material behavior (Nasr et al., 2025). Korat et al. (2025) successfully incorporated finely crushed ceramic waste into ultra-high-performance concrete (UHPC), achieving compressive strengths exceeding 170 MPa at a 20% replacement level under the investigated UHPC formulation. This performance was associated with enhanced particle packing, secondary hydration product formation, and interfacial transition zone (ITZ) refinement (Korat et al., 2025). Meanwhile, Tang (2025) investigated stray-current-induced corrosion in SFRC, demonstrating that chloride concentration and fiber orientation significantly influenced electrochemical behavior and corrosion susceptibility. These findings emphasized the importance of considering environmental exposure and fiber–matrix interactions when evaluating fiber-reinforced cementitious composites (Tang, 2025).

A critical synthesis of the available literature reveals that the effectiveness of WCP is governed by competing physical and chemical mechanisms. Moderate replacement levels, particularly within the range of 10–20%, frequently provide satisfactory mechanical performance through

filler effects, heterogeneous nucleation, and potential pozzolanic reactions. Conversely, excessive replacement generally leads to cement dilution and insufficient hydration product formation. Moreover, contradictory findings regarding water absorption indicate that WCP-induced changes in pore structure and matrix compactness are highly dependent on material characteristics and mixture proportions. Although SFs substantially improve tensile and flexural performance through crack bridging, their effectiveness depends on fiber dispersion, interfacial bonding, and the mechanical integrity of the surrounding matrix.

From a mechanistic perspective, combining WCP and SFs represents a potentially complementary multiscale modification strategy. At the microscale, reactive siliceous and aluminous constituents of WCP may interact with calcium hydroxide released during cement hydration, contributing to additional calcium silicate hydrate (C–S–H) and calcium aluminosilicate hydrate (C–A–S–H) formation. These mechanisms may refine the pore structure and improve the ITZ surrounding aggregates and fibers. At the macroscale, SFs restrict crack propagation, redistribute tensile stresses, and enhance resistance to progressive fracture. However, excessive WCP replacement may weaken fiber anchorage through cement dilution, whereas excessive fiber incorporation may adversely affect workability, dispersion, and matrix compactness. Consequently, the combined effects of WCP and SFs are expected to exhibit nonlinear and potentially competing interactions rather than universally beneficial behavior.

Despite extensive research on WCP-modified concrete and SFRC independently, the reviewed literature provides limited systematic evidence regarding their coupled effects on age-dependent mechanical performance and water absorption. In particular, the extent to which SFs can compensate for mechanical deterioration associated with increasing WCP content while maintaining satisfactory water absorption remains insufficiently characterized. Furthermore, previous investigations have predominantly focused on individual material optimization or prediction of specific mechanical properties, with comparatively limited attention to integrated experimental and nonlinear modeling frameworks addressing multiple performance indicators simultaneously.

To address these research gaps, the present study systematically investigates the individual and interactive effects of WCP and SFs on the mechanical performance and water absorption behavior of sustainable concrete. A comprehensive experimental program comprising 15 concrete mixtures was designed using five WCP replacement levels (0, 10, 20, 30, and 40% by cement mass) and three SF volume fractions (0, 0.75, and 1.5%). Compressive strength was evaluated at 7, 14, 28, and 90 days, while splitting tensile strength, flexural strength, and water absorption were determined at 90 days.

Furthermore, third-order polynomial regression, response surface analysis, and Pearson correlation analysis were employed to characterize nonlinear relationships between mixture composition and performance indicators. The principal novelty of this investigation lies in

integrating age-dependent experimental characterization with multivariable modeling to evaluate the potential complementary effects of ceramic waste-derived matrix modification and steel fiber reinforcement. By identifying the trade-offs between cement replacement, mechanical performance, and water absorption, this study provides a systematic basis for developing resource-efficient cementitious composites and optimizing sustainable concrete mixtures within the investigated experimental domain.

2. Materials and Methods

2.1. Aggregates

In this study, crushed mountain aggregates were employed as the primary mineral constituents of the concrete mixture, with both the fine and coarse aggregate fractions sourced entirely from quarry derived materials. The use of crushed mountain aggregates, characterized by their angular shape, rough surface texture, and high mechanical strength, plays a critical role in enhancing the overall performance of the concrete. The angularity of these aggregates improves interlocking within the matrix, resulting in superior load transfer mechanisms and reduced internal slippage under mechanical stresses. Additionally, the rough surface morphology promotes stronger adhesion between the aggregates and the cementitious paste, thereby increasing the tensile and compressive strength of the composite material.

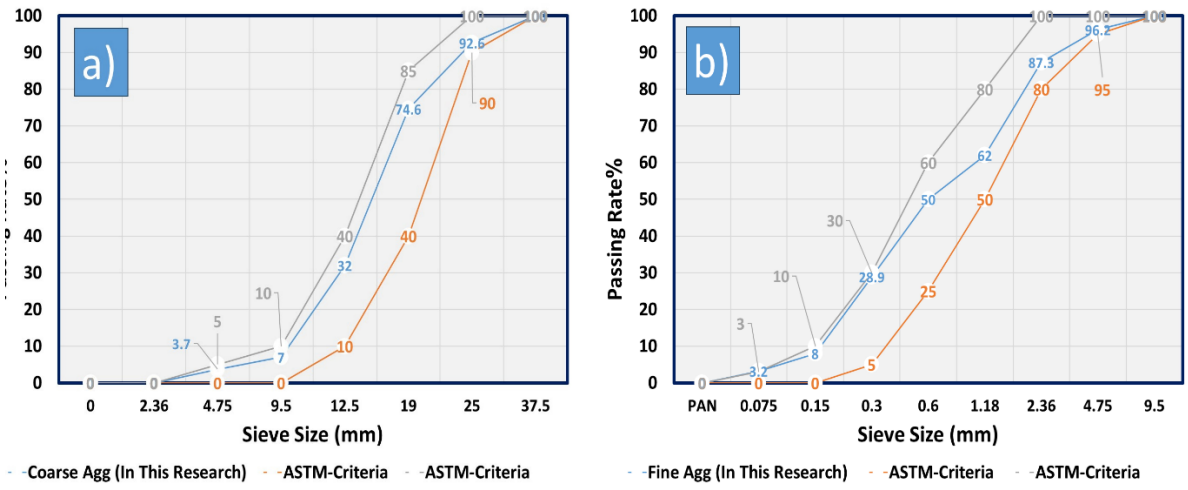

Figure 1. Comparison of the particle-size distribution of the coarse and fine aggregates used in this study with ASTM specification ranges.

The results of the sieve analysis of the aggregates used in this study are presented in Figure 1, which is divided into two parts: (a) coarse aggregates and (b) fine aggregates. These plots illustrate the cumulative percent passing as a function of sieve size, and the reference limits

shown correspond to the permissible ranges specified in ASTM C33/C33M, the primary standard governing aggregate requirements for concrete (ASTM, 2023).

In part (a), the gradation curve of the coarse aggregates falls entirely within the acceptable limits defined by ASTM C33/C33M across all standard sieve sizes. The uniform distribution of percent passing and the smooth continuity of the curve indicate that the material possesses a well-graded particle-size distribution without any signs of gap grading. According to the standard requirements, such a continuous gradation is essential for achieving optimal packing density, reducing void content, and improving the mechanical performance of concrete. Furthermore, compliance with the specified limits confirms that the nominal maximum size and the amount of fine particles within the coarse aggregate fraction are properly controlled.

In part (b), the gradation of the fine aggregates also conforms to the ASTM C33/C33M limits (ASTM, 2023). The percent passing through the finer sieves, particularly the 0.15 mm and 0.30 mm sizes, falls within the acceptable range, indicating adequate control of very fine particles and preventing excessive water demand in the mixture. This compliance contributes to improved workability, reduced shrinkage potential, and enhanced durability of the concrete.

Overall, the conformity of both coarse and fine aggregate gradation curves with the ASTM C33/C33M specification demonstrates that the aggregates used in this study meet the required particle-size distribution criteria necessary for producing concrete with reliable quality and satisfactory performance.

2.2. WCP, SFs and Cement

In this study, two key additives, WCP and SFs, were incorporated to enhance the mechanical performance and stability of the concrete mixtures. These materials, illustrated in Figure 2, align with modern civil engineering approaches that simultaneously promote the recycling of industrial waste and the improvement of structural performance.



Figure 2. WCP and SFs used in this study

The left section of Figure 2 shows the WCP. This material, produced by crushing and grinding recycled ceramic waste, has a fine, powder-like texture. In concrete engineering, WCP, owing to its potential pozzolanic characteristics when properly processed, can partially replace cement or act as a filler to refine the pore structure of the concrete matrix. Beyond its technical benefits, the use of WCP contributes to environmental sustainability by reducing cement consumption, lowering production costs, and minimizing greenhouse gas emissions associated with cement manufacturing.

The right section of the figure displays the SF, which appear as short, slender metallic filaments. Due to their high tensile strength, SFs are widely used as secondary reinforcement in concrete. Their primary role is to control cracking, enhance ductility, improve impact resistance, and limit the propagation of microcracks. The presence of SFs within the concrete matrix introduces a bridging mechanism that prevents crack widening, thereby improving post-cracking behavior and increasing the toughness of the composite material.

Overall, the combined use of WCP as a micro-level enhancement material and SF as a macro-level reinforcing element represents a comprehensive approach aimed at producing concrete with improved durability, superior mechanical performance, and enhanced environmental characteristics. The scale indicators shown in the figure provide a reference for the physical dimensions of these materials, ensuring quality control and verification of their technical specifications prior to mixing.

2.3. Chemical Composition of WCP and Cement

According to Table.1, the chemical oxide composition of the Type II Ardestan cement and the WCP demonstrates a complementary behavior that supports pozzolanic activity within the blended system. The WCP contains a remarkably high proportion of SiO_2 (67%) and Al_2O_3 (19.5%), which together exceed 70%, placing it well within the typical compositional range of natural and artificial pozzolans. Its low CaO content (2.1%) further confirms that WCP behaves primarily as a reactive siliceous–aluminous material rather than a cementitious one, relying on calcium hydroxide released during cement hydration to form additional C–S–H gel.

Table 1. Chemical oxide composition of the WCP and Portland cement used in this study.

Compounds	SiO_2	Al_2O_3	Fe_2O_3	CaO	MgO	Na_2O	TiO_2	K_2O	SO_3	L.O.I
WCP	67	19.5	0.5	2.1	0.85	3.9	0.25	2.3	0.3	3
Cement	22.1	5	4	64	1.2	0.35	<0.1	0.65	2.1	0.5

In contrast, the Type II Ardestan cement listed in Table 2 contains 64% CaO, consistent with Portland cement chemistry, along with moderate amounts of SiO_2 and Al_2O_3. This high calcium content provides the necessary environment for secondary pozzolanic reactions when blended with WCP. The low L.O.I values for both materials indicate minimal impurities and good thermal stability. Overall, the oxide composition presented in Table 1 confirms that WCP falls within the pozzolanic range and can effectively enhance long term strength and durability when combined with Type II Ardestan cement.

2.4. Water and Superplasticizer

In this study, potable water was used for all mixing and curing operations to ensure chemical purity, consistency, and full compliance with international standards governing concrete production. The use of drinking quality water eliminates the presence of harmful ions such as chlorides, sulfates, or organic contaminants that could otherwise interfere with cement hydration or adversely affect the long-term durability of the composite material. Potable water provides a stable environment for the formation of primary hydration products, particularly C–S–H gel, which governs the mechanical performance of cementitious systems.

Additionally, a lignosulfonate-based superplasticizer was incorporated into the mixture to enhance workability without increasing the water to cement ratio. Lignosulfonate admixtures function primarily through electrostatic dispersion, reducing the surface tension of water and improving the separation of cement particles. This mechanism leads to improved flowability, better compaction, and reduced entrapped air, ultimately contributing to higher density and improved mechanical properties. The use of this superplasticizer also supports more efficient hydration by facilitating uniform water distribution throughout the matrix. Overall, the combined use of potable water and a lignosulfonate superplasticizer ensures optimal fresh state behavior and contributes to the development of a durable, high performance concrete mixture in this research.

2.5. Concrete Mix Design

In Table. 2, the concrete mix designs were developed to investigate the simultaneous effects of replacing cement with WCP and incorporating SF on the properties of concrete. A total of 15 mix designs were considered in this experimental program, derived from the combination of five replacement levels of WCP and three dosage levels of SF. In all mixtures, the aggregate contents were kept constant, with fine aggregate fixed at 827 kg/m³ and coarse aggregate at 1010 kg/m³. Likewise, the water content was maintained at 160 L/m³ for all mixes, and the water-to-cement ratio was kept constant at 0.40 to ensure reliable comparison of the results. The dosage of the superplasticizer was also fixed at 8 kg/m³ across all mixtures to preserve the workability of fresh concrete in the presence of WCP and SF. In this mix design, the total cementitious material content (cement plus WCP) was kept constant at 400 kg/m³ for all specimens, with only the proportion between the two materials varying.

To examine the influence of cement replacement with WCP, five replacement levels were selected: 0%, 10%, 20%, 30%, and 40% by weight of cement. Accordingly, in the control mixture (0% replacement), the cement content was 400 kg/m³ with no WCP. As the replacement level increased, the cement content decreased to 360, 320, 280, and 240 kg/m³, while the corresponding WCP contents increased to 40, 80, 120, and 160 kg/m³, respectively. In addition, to evaluate the role of SF in enhancing the mechanical behavior of concrete, three fiber volume fractions (0%, 0.75%, and 1.5%) were incorporated. These correspond to fiber dosages of 0, 58.5, and 117 kg/m³ of concrete, respectively. Therefore, for each WCP replacement level, three mixtures with different SF contents were prepared, resulting in a matrix of 15 mix designs.

The naming system adopted for the mix designs was structured such that the proportions of WCP and SF could be directly inferred from the mix label. In this system, the letter W denotes the percentage of cement replaced by WCP, and SF represents the percentage of SFs. The numerical value following each letter indicates the corresponding percentage used in the mixture. For example, the designation W0%SF0% indicates that neither WCP nor SF were used, and this mixture serves as the control specimen. The label W10%SF0.75% indicates a mixture containing 10% cement replacement with WCP and 0.75% SF. Similarly, W20%SF1.5% represents a mixture with 20% WCP and 1.5% SF. This systematic naming approach facilitates straightforward identification of each mix composition and enables structured comparison among the mixtures. Overall, the adopted naming and mix design framework allows for a comprehensive evaluation of the individual and combined effects of WCP and SF on the mechanical and durability performance of concrete.

Table 2. Concrete mix design

Mix ID	Fine Aggregate (kg/m³)	Coarse Aggregate	Cement (kg/m³)	SF (kg/m³)	WCP (kg/m³)	Water-to-Binder Ratio	Water (L/m³)	Superplasticizer (kg/m³)

W0%SF0%	827	1010	400	0	0	0.4	160	8
W0%SF0.75%	827	1010	400	58.5	0	0.4	160	8
W0%SF1.5%	827	1010	400	117	0	0.4	160	8
W10%SF0%	827	1010	360	0	40	0.4	160	8
W10%SF0.75%	827	1010	360	58.5	40	0.4	160	8
W10%SF1.5%	827	1010	360	117	40	0.4	160	8
W20%SF0%	827	1010	320	0	80	0.4	160	8
W20%SF0.75%	827	1010	320	58.5	80	0.4	160	8
W20%SF1.5%	827	1010	320	117	80	0.4	160	8
W30%SF0%	827	1010	280	0	120	0.4	160	8
W30%SF0.75%	827	1010	280	58.5	120	0.4	160	8
W30%SF1.5%	827	1010	280	117	120	0.4	160	8
W40%SF0%	827	1010	240	0	160	0.4	160	8
W40%SF0.75%	827	1010	240	58.5	160	0.4	160	8
W40%SF1.5%	827	1010	240	117	160	0.4	160	8

Figure 3 illustrates the comprehensive, step by step process of preparing, casting, demolding, and curing the concrete specimens in the laboratory, together with the visual characteristics and scale of the novel materials employed in this research. It presents the experimental framework of the study in the form of a continuous and integrated graphical workflow. In the upper part of this figure, the laboratory production sequence of the specimens is depicted. In the first stage (top left image), the fresh concrete containing the different mix designs, after completion of the mixing process, is poured into standard cubic molds (for compressive strength determination) and prismatic molds (for flexural strength testing). The molds are then placed on a vibrating table to achieve maximum compaction and to expel entrapped air voids. The identification labels attached to the molds indicate the precise coding of the specimens, enabling clear distinction between the various experimental variables. In the second stage (top right image), the demolding (decoupage) process is carried out after the first 24 hours from casting, once initial setting has been achieved. The hardened specimens, maintaining full structural integrity and free from edge spalling or cracking, are removed from the steel and plastic molds and neatly arranged in preparation for the curing phase. In the third stage (bottom image of the first section), these concrete specimens are placed in a water curing tank under fully submerged conditions so that cement hydration and secondary reactions can proceed under saturated moisture and standard room temperature. This stage is critical for the formation of calcium silicate hydrate gel (C–S–H), for reducing permeability, for preventing plastic shrinkage cracking, and ultimately for achieving the target mechanical strength at different ages, particularly at 7,14,28 and 90 days.

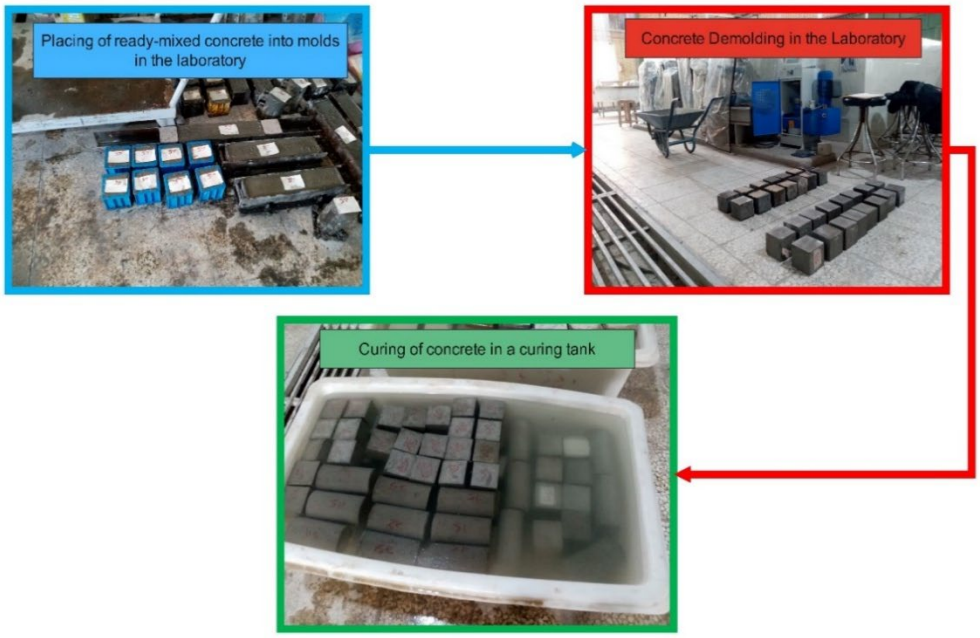

Figure 3. Step by step process of preparing, casting, demolding, and curing the concrete specimens in the laboratory

2.6. Testing Methodology for Mechanical and Durability Properties

In this study, a comprehensive experimental program was designed to evaluate the mechanical performance and durability characteristics of the concrete mixtures at various curing ages. The compressive strength development was examined using 10×10×10 cm cubic specimens, tested at 7, 14, 28, and 90 days. These testing intervals were selected to capture the evolution of strength from early hydration stages through intermediate microstructural refinement and into long term maturity. The compressive strength results provide critical insight into the progression of load carrying capacity and the influence of material composition on hydration kinetics and microstructural densification.

To assess the tensile behavior of the concrete, indirect tensile strength tests were conducted at 90 days following the Brazilian splitting test method. For this purpose, cylindrical specimens with a diameter of 10 cm and a height of 20 cm were utilized. The Brazilian test induces tensile stresses perpendicular to the applied compressive load, enabling an indirect yet reliable measurement of the material's tensile resistance. This parameter is essential for understanding crack initiation, propagation mechanisms, and the overall brittleness of cementitious composites (ASTM, 2021).

Furthermore, the flexural strength of the concrete was evaluated at 90 days using 10×10×50 cm prismatic beams subjected to the three-point bending test. This test configuration provides valuable information regarding the modulus of rupture and the material's ability to withstand

bending stresses, which is particularly relevant for structural elements such as beams, slabs, and pavements where flexural performance governs serviceability and failure modes.

Beyond mechanical characterization, the durability of the concrete was also investigated. After reaching 90 days of curing, the 10 cm cubic specimens were immersed in water for 72 hours to determine their water absorption capacity, a key indicator of permeability and long-term durability. The water absorption test quantifies the degree of pore connectivity and the susceptibility of the concrete to moisture ingress, which directly influences its resistance to freeze–thaw cycles, chloride penetration, sulfate attack, and other degradation mechanisms. By comparing the dry and saturated masses of the specimens, the percentage of absorbed water was calculated, providing a measure of microstructural integrity and the effectiveness of the binder system in reducing capillary porosity. Collectively, the compressive, tensile, and flexural strength tests, along with the water absorption assessment, offer a holistic evaluation of the concrete's mechanical behavior and durability performance. This integrated testing framework enables a robust understanding of how the material responds to different loading conditions and environmental exposures, thereby supporting a comprehensive assessment of its suitability for long term structural applications.

2.7. Third-Order Polynomial Regression and Pearson Correlation Analysis

In this study, a third-degree regression approach was adopted to model the relationship between the mix input parameters, WCP content and SFs, and the measured performance responses of the concrete specimens. The purpose of using this statistical method was to obtain empirical equations capable of capturing nonlinear trends and combined effects of the two variables on the investigated properties.

The experimental matrix consisted of mixtures prepared with different levels of WCP (used as a partial replacement material) and various dosages of SFs (added as discrete reinforcement). The response variables included compressive strength at 7, 14, 28, and 90 days, as well as splitting tensile strength, flexural strength, and water absorption measured on 90-day specimens. These outputs were selected to represent both early-age and long-term strength development and to evaluate mechanical behavior under tension/flexure together with durability-related performance.

Because the effect of WCP content and SFs in cement-based systems is often not purely linear, due to mechanisms such as filler/packing effects, changes in hydration products, fiber dispersion limits, and crack-bridging behavior, a cubic (third-order) polynomial regression model was selected. Compared with linear and quadratic models, a third-degree model provides greater flexibility to represent curvature, turning points, and interaction-related behavior across the range of the investigated parameters (Gaffke & Heiligers, 1996).

For each response variable, a separate third-order regression equation was developed using the experimental dataset. The general form of the model is given in Eq. (1):

$$Z = p_0 + p_1X + p_2Y + p_3X^2 + p_4Y^2 + p_5XY + p_6X^3 + p_7Y^3 + P_8X^2Y + P_9XY^2 \quad (1)$$

where Z is the predicted output (compressive strength at a given curing age, 90-day splitting tensile strength, 90-day flexural strength, or 90-day water absorption), X denotes the WCP content, Y denotes the SFs dosage and p0 to p9 are regression coefficients. The regression coefficients were estimated by the least-squares method, ensuring minimization of the overall difference between measured and predicted values. Model adequacy was assessed using common statistical indicators such as the coefficient of determination (R^2), adjusted R^2, and evaluation of residual behavior to confirm that the cubic regression form can reasonably represent the experimental data within the investigated domain.

In addition to regression modeling, Pearson correlation analysis was performed to evaluate the degree and statistical significance of the relationships between the input parameters and the outputs. Pearson correlation coefficients were computed between each input variable (tile powder waste content and steel fiber dosage) and each measured response (compressive strengths at 7, 14, 28, and 90 days, as well as 90-day splitting tensile strength, flexural strength, and water absorption). The corresponding p-values were used to determine the significance of the observed correlations, providing an initial indication of which input–output relationships are statistically meaningful and whether the association is positive or negative. This correlation-based screening supported the interpretation of the regression outcomes by highlighting the most influential parameters for each performance metric.

All regression and correlation analyses were conducted in MATLAB, enabling systematic data processing, coefficient estimation, statistical evaluation, and comparison between predicted and experimental results. Overall, combining third-order polynomial regression with Pearson significance testing provided a robust framework for explaining the experimental behavior of the cement-based specimens and for developing empirical predictive relationships that can be used in mixture design and optimization.

3. Results

3.1. Compressive Strength

Based on the results presented in Figure 4, the compressive strength development of concrete incorporating waste ceramic powder (WCP) and steel fibers (SFs) at 7, 14, 28, and 90 days appears to be governed by the competing contributions of cement dilution, particle packing, potential pozzolanic activity, and fiber-induced modifications of the cementitious matrix. In the control mixture (W0%SF0%), compressive strength increased from 26.04 MPa at 7 days to

39.61 MPa at 90 days, reflecting the progressive hydration of Portland cement and the accumulation of calcium silicate hydrate (C–S–H), which is primarily responsible for strength development. When 10% of the cement was replaced with WCP (W10%SF0%), a slight reduction in early-age compressive strength was observed; however, the 90-day strength reached 40.04 MPa, approximately 1.09% higher than that of the control mixture. This marginal improvement may be associated with the combined contributions of the physical filler effect, heterogeneous nucleation, and potential secondary pozzolanic reactions between the reactive siliceous constituents of WCP and calcium hydroxide ($Ca(OH)_2$) released during cement hydration. This interpretation is consistent with the findings of Li et al. (2020), who demonstrated the potential of ceramic powder to function as both a supplementary filler and a pozzolanic material in cementitious systems (Li et al., 2020). Similarly, Kannan et al. (2017) emphasized that the contribution of WCP to concrete performance may be predominantly governed by its physical filler effect rather than its pozzolanic reactivity, highlighting the importance of particle packing and matrix densification (Kannan et al., 2017).

Increasing the WCP replacement level to 20% (W20%SF0%) reduced the 90-day compressive strength to 36.28 MPa, corresponding to an 8.41% reduction relative to the control mixture. At replacement levels of 30% and 40%, the corresponding compressive strengths decreased to 33.00 and 33.32 MPa, representing reductions of approximately 16.69% and 15.88%, respectively. These results suggest that the cement dilution effect progressively outweighs the beneficial contributions of particle packing and potential pozzolanic activity at higher replacement levels. The reduction in Portland cement content limits the formation of primary hydration products and may also restrict the availability of calcium hydroxide required for secondary pozzolanic reactions. Nevertheless, the relative strength gain between 7 and 90 days exceeded 60% in mixtures containing higher WCP contents, compared with approximately 52.11% for the control mixture. Although this higher relative strength development partly reflects the lower initial strength of WCP-modified mixtures, it may also indicate delayed contributions from ceramic particles to matrix refinement. These observations are broadly consistent with Heidari and Tavakoli (2013), who reported that moderate WCP replacement levels could maintain satisfactory long-term compressive strength despite reductions at early curing ages (Heidari & Tavakoli, 2013). Accordingly, the present findings suggest that the effectiveness of WCP is strongly dependent on the balance between replacement level, curing duration, and the physical and chemical characteristics of the ceramic particles.

Regarding the influence of SFs, incorporating a fiber volume fraction of 0.75% into the reference mixture (W0%SF0.75%) reduced the 90-day compressive strength to 38.85 MPa, corresponding to a marginal reduction of approximately 1.92%. A slightly greater reduction was observed at a fiber volume fraction of 1.5%. These reductions may be associated with decreased workability, nonuniform fiber dispersion, entrapped air, and localized disturbances in matrix compactness. Unlike WCP, the primary contribution of SFs is mechanical rather than cementitious, principally involving crack bridging, stress redistribution, and restriction of crack

propagation. Consequently, their beneficial effects are generally more pronounced under tensile and flexural loading than under compression. Comparable observations were reported by Alegre Cornelio et al. (2024), who found that the simultaneous incorporation of 10% ceramic powder and 1.5% steel fibers resulted in a 4% reduction in compressive strength, despite improvements of 8.5% and 3% in tensile and flexural strengths, respectively (Cornelio et al., 2024). These findings support the interpretation that fiber reinforcement does not necessarily enhance compressive strength, particularly when its incorporation adversely affects the physical integrity of the surrounding matrix.

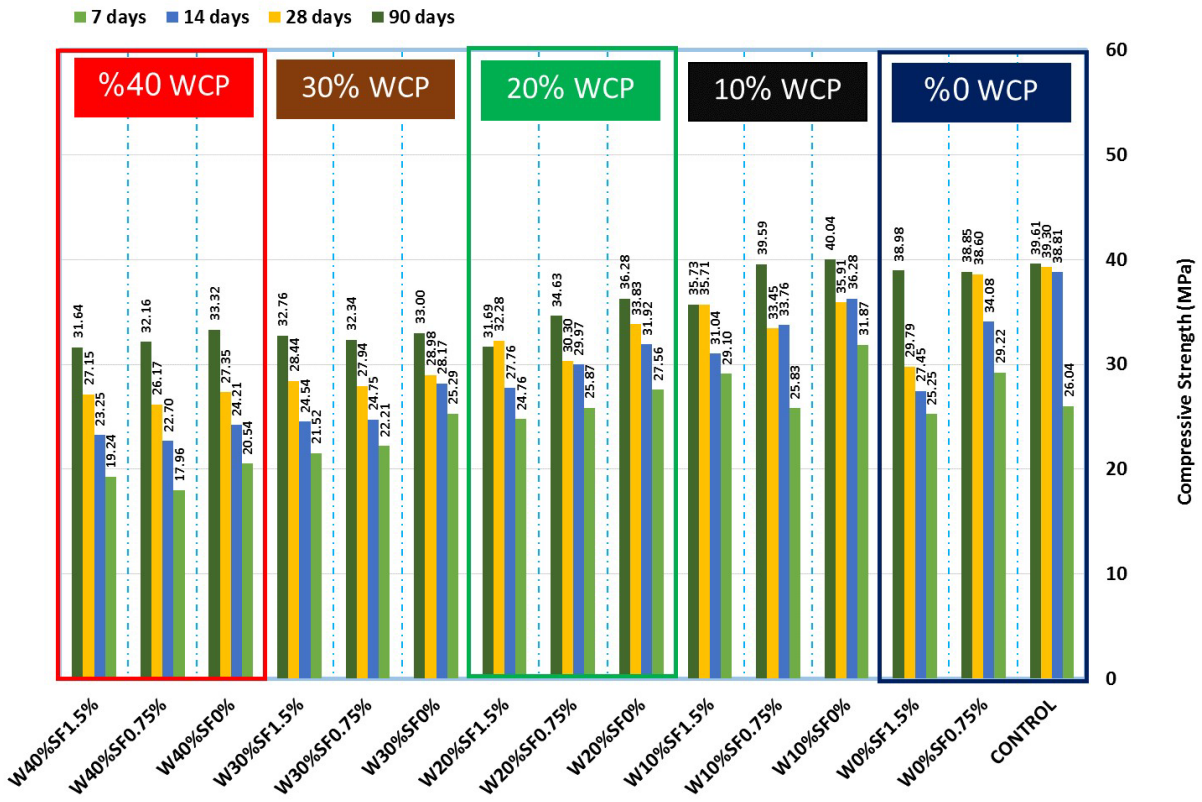

Figure 4. The compressive strength test results of the 10×10 cm cubic specimens at different curing ages.

The simultaneous incorporation of WCP and SFs revealed a composition-dependent interaction between binder modification and mechanical reinforcement. In particular, the mixture W10%SF0.75% achieved a 90-day compressive strength of 39.59 MPa, representing approximately 99.95% of the control strength while reducing Portland cement consumption by 10%. This result suggests that the beneficial physical and potential chemical contributions of moderate WCP incorporation may compensate for the minor reduction in matrix compactness associated with fiber addition. However, at a WCP replacement level of 20%, the incorporation of 0.75% SFs was insufficient to fully compensate for the strength reduction associated with cement dilution. Furthermore, mixtures containing higher fiber dosages, particularly W20%SF1.5% and W40%SF1.5%, exhibited more pronounced early-age strength reductions, potentially reflecting the combined effects of reduced cement content, lower workability, and

unfavorable fiber dispersion. The subsequent strength recovery observed at later curing ages may be related to continued cement hydration, progressive pore refinement, and potential secondary pozzolanic reactions, as supported by the mechanisms discussed by Kannan et al. (2017) and Li et al. (2020) (Kannan et al., 2017; Li et al., 2020).

Overall, the compressive strength results indicate that moderate WCP replacement provides a favorable balance between cement reduction and mechanical performance, whereas excessive replacement leads to strength deterioration dominated by cement dilution. Although SFs provide effective mechanical reinforcement, their contribution to compressive strength remains limited and depends on the quality of the surrounding cementitious matrix. Among the investigated compositions, W10%SF0.75% represents a technically favorable mixture from the perspective of compressive strength retention and reduced cement consumption. Nevertheless, the proposed microstructural and chemical mechanisms should be regarded as plausible interpretations of the experimental trends rather than directly verified phenomena, given the absence of dedicated microstructural and mineralogical characterization.

Overall, the analysis of Figure 4 reveals that the optimal performance occurs when the amount of $Ca(OH)_2$ produced by cement hydration is sufficient to activate WCP, but not so limited that the dilution effect becomes dominant. Accordingly, the mixture W10%SF0.75% emerges as the most balanced option, as it promotes effective secondary C–S–H formation, maintains compressive strength, and significantly reduces cement consumption. This combination represents the most favorable synergy between chemical and mechanical mechanisms, offering a sustainable mixture design with robust long-term performance.

3.2. Flexural Strength

The 90-day flexural strength results presented in Figure 5 reveal a highly instructive interaction between the pozzolanic activity of waste ceramic powder and the mechanical bridging contribution of SFs, demonstrating how these two parameters collectively govern the tensile load carrying capacity and post cracking behavior of the composite system under three-point bending. As the data indicate, mixtures incorporating waste ceramic powder without SFs show a progressive increase in flexural strength from 0% to 30% replacement, rising from 2.34 MPa to 3.86 MPa, before declining to 2.93 MPa at 40% replacement; this trend is consistent with the expected behavior of a pozzolanic material that contributes to long term strength development through secondary hydration reactions. At 90 days, the pozzolanic reaction between the amorphous aluminosilicate phases in the ceramic powder and the calcium hydroxide liberated during cement hydration leads to the formation of additional C–S–H and C–A–S–H gels, which refine the pore structure, densify the matrix, and enhance the tensile resistance of the composite; this mechanism is well aligned with established models of secondary C–S–H formation and microstructural densification. The strength reduction at 40% replacement suggests that the binder system becomes under cemented, meaning that the available $Ca(OH)_2$ is insufficient to fully react with the pozzolanic material, resulting in a less

cohesive matrix and a weaker interfacial transition zone (ITZ). When SFs are introduced, the flexural strength increases dramatically across all replacement levels, with the 0% ceramic mixture rising from 2.34 MPa to 5.33 MPa and 6.32 MPa at 0.75% and 1.5% fiber content, respectively; this improvement is attributed to the crack bridging action of the fibers, which enhances post cracking load capacity, delays macrocrack propagation, and increases the energy absorption capacity of the composite.

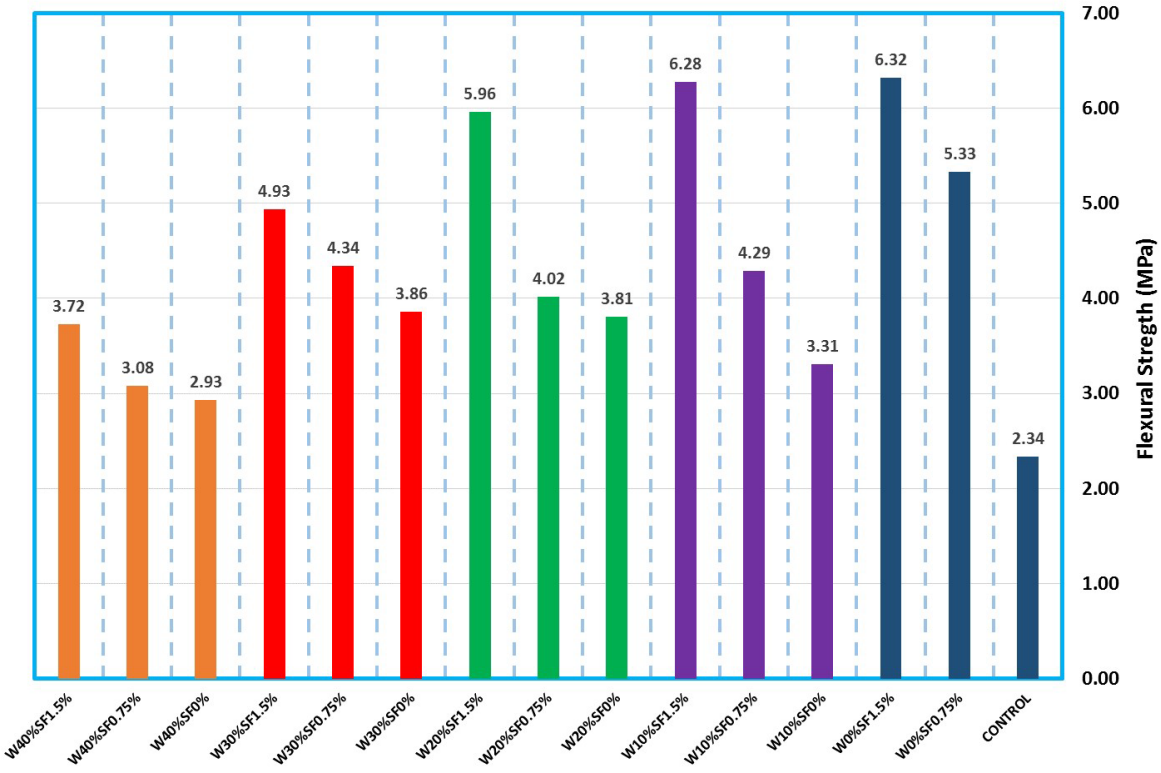

Figure 5. The flexural strength test results at 90n days curing ages.

The effectiveness of SFs is governed by the fiber–matrix bond, pull out resistance, and fiber dispersion, all of which are improved at 90 days due to the denser matrix produced by ongoing hydration and pozzolanic reactions. The combined effect of waste ceramic powder and SFs is particularly noteworthy: at moderate replacement levels (10% and 20%), the flexural strengths of mixtures containing 1.5% steel fiber reach 6.28 MPa and 5.96 MPa, values comparable to the 0% ceramic mixture with the same fiber content, indicating that the pozzolanic matrix provides a stronger microstructure for fiber anchorage while the fibers compensate for the increased brittleness typically associated with ceramic replacement. This synergy is explained by the improved ITZ, where the reduction of portlandite crystals and the formation of secondary C–S–H enhance the mechanical interlock between the fibers and the matrix, increasing the resistance to pull out and improving crack deflection behavior; this aligns with established theories of fiber–matrix interlock and ITZ strengthening. However, at higher replacement levels (30% and 40%), the flexural strength of fiber reinforced mixtures declines

to 4.93 MPa and 3.72 MPa, respectively, due to the reduced cement content and insufficient $Ca(OH)_2$ to sustain a robust pozzolanic reaction, leading to a weaker matrix that cannot fully mobilize the bridging capacity of the fibers. Despite this reduction, the presence of fibers still significantly improves performance relative to fiber free mixtures, demonstrating that fiber reinforcement remains effective even when the matrix is suboptimal. From a microstructural perspective, the pozzolanic reaction contributes to matrix densification and ITZ improvement, reducing porosity and enhancing the mechanical anchorage of fibers, which in turn increases the composite's ability to resist crack initiation and propagation. The failure mode transitions from brittle in plain mixtures to ductile in fiber reinforced mixtures, with fibers bridging microcracks, delaying macrocrack formation, and enabling the composite to sustain higher loads after initial cracking; this behavior is consistent with established models of ductility enhancement in fiber reinforced composites. Overall, the results in Figure 5 clearly demonstrate that waste ceramic powder enhances flexural strength up to 30% replacement through pozzolanic activity, SFs significantly increase flexural performance through crack bridging and energy absorption mechanisms, and the combination of moderate ceramic replacement (10–20%) with 1.5% steel fiber yields the most favorable balance between sustainability, microstructural refinement, and mechanical performance. These findings underscore the potential of integrating pozzolanic ceramic waste with steel fiber reinforcement to produce high performance, environmentally optimized cementitious composites with superior flexural behavior at advanced curing ages.

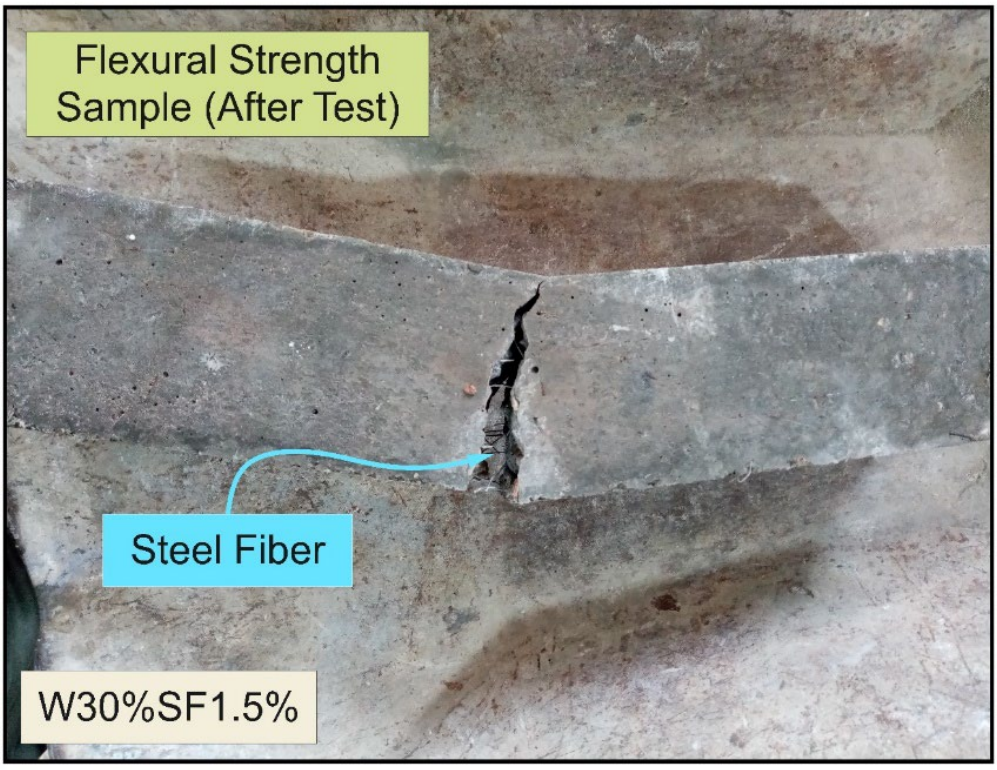

Figure 6. Post failure condition of the flexural specimen

The post failure condition of the flexural specimen shown in Figure 6 provides critical insight into the mechanical response of the composite under bending and highlights the combined influence of waste ceramic powder and SFs on crack propagation, energy absorption, and residual load carrying capacity. The visible central crack, accompanied by the protruding SFs bridging the fracture plane, confirms that the failure mode is governed not by sudden brittle rupture but by a progressive crack opening mechanism characteristic of fiber reinforced cementitious composites. In the W30%SF1.5% mixture, the presence of 30% waste ceramic powder contributes to a refined microstructure through its pozzolanic reaction, which enhances matrix density and improves the interfacial transition zone (ITZ) around both aggregates and fibers. This densification increases the mechanical anchorage of the SFs, enabling them to engage more effectively during crack initiation and propagation. As the flexural load increases, microcracks form within the matrix but are delayed in coalescing into a dominant macrocrack due to the crack bridging action of the fibers. Once the main crack forms, the fibers crossing the fracture plane undergo a combination of pull out and tensile rupture, dissipating significant energy and providing a residual flexural capacity even after matrix failure. The exposed fibers in the image clearly illustrate this mechanism: some fibers remain partially embedded, indicating strong bond strength, while others appear stretched or bent, reflecting the high frictional resistance mobilized during pull out.

The ceramic modified matrix, although slightly weaker than pure cement paste at high replacement levels, still provides sufficient bonding to activate the fibers' bridging potential, which explains why the W30%SF1.5% mixture maintains a relatively high flexural strength despite reduced cement content. The crack pattern also suggests that the failure was not catastrophic; instead, the specimen experienced a controlled, ductile response, consistent with the behavior expected from composites designed for enhanced toughness. This observation aligns with the mechanical trends reported earlier, where mixtures containing both ceramic powder and SFs exhibited improved post cracking performance compared to fiber free systems. The specimen's behavior in Figure 6 therefore validates the synergistic interaction between the pozzolanic matrix and the reinforcing fibers: the ceramic powder contributes to microstructural refinement and improved ITZ quality, while the fibers provide ductility, crack control, and enhanced energy absorption. Together, these mechanisms produce a composite capable of sustaining significant deformation after initial cracking, making it suitable for structural applications where flexural toughness and durability are critical. Overall, the visual evidence in Figure 6 reinforces the mechanical results and confirms that the W30%SF1.5% mixture exhibits a balanced combination of strength, ductility, and crack resistance due to the complementary roles of pozzolanic reaction and fiber reinforcement.

3.3. Tensile Strength

The 90-day Brazilian tensile strength results presented in Figure 7 provide a comprehensive understanding of how the combined effects of waste-ceramic powder as a partial cement

replacement and steel fiber reinforcement influence the indirect tensile behavior of the composite, revealing the complex interplay between matrix chemistry, microstructural evolution, and fiber-bridging mechanisms under diametral compression. The data show that in mixtures without SFs, the tensile strength initially decreases slightly with the incorporation of ceramic powder, dropping from 3.30 MPa at 0% replacement to 3.12 MPPa at 10% and 3.23 MPa at 20%, before rising to 3.48 MPa at 30% and then declining again to 3.05 MPa at 40%; this pattern reflects the characteristic behavior of a pozzolanic material whose contribution to strength becomes more pronounced at later ages due to the gradual formation of secondary hydration products. At 90 days, the amorphous aluminosilicate phases in the ceramic powder react with calcium hydroxide released during cement hydration, producing additional C–S–H and C–A–S–H gels that densify the matrix, refine pore structure, and strengthen the interfacial transition zone (ITZ). This microstructural refinement explains why the tensile strength at 30% replacement surpasses that of the 10% and 20% mixtures, as the pozzolanic reaction becomes sufficiently advanced to compensate for the reduction in clinker content. However, at 40% replacement, the tensile strength declines again, indicating that the system becomes under-cemented, with insufficient $Ca(OH)_2$ available to sustain a robust pozzolanic reaction, resulting in a weaker matrix and reduced crack resistance.

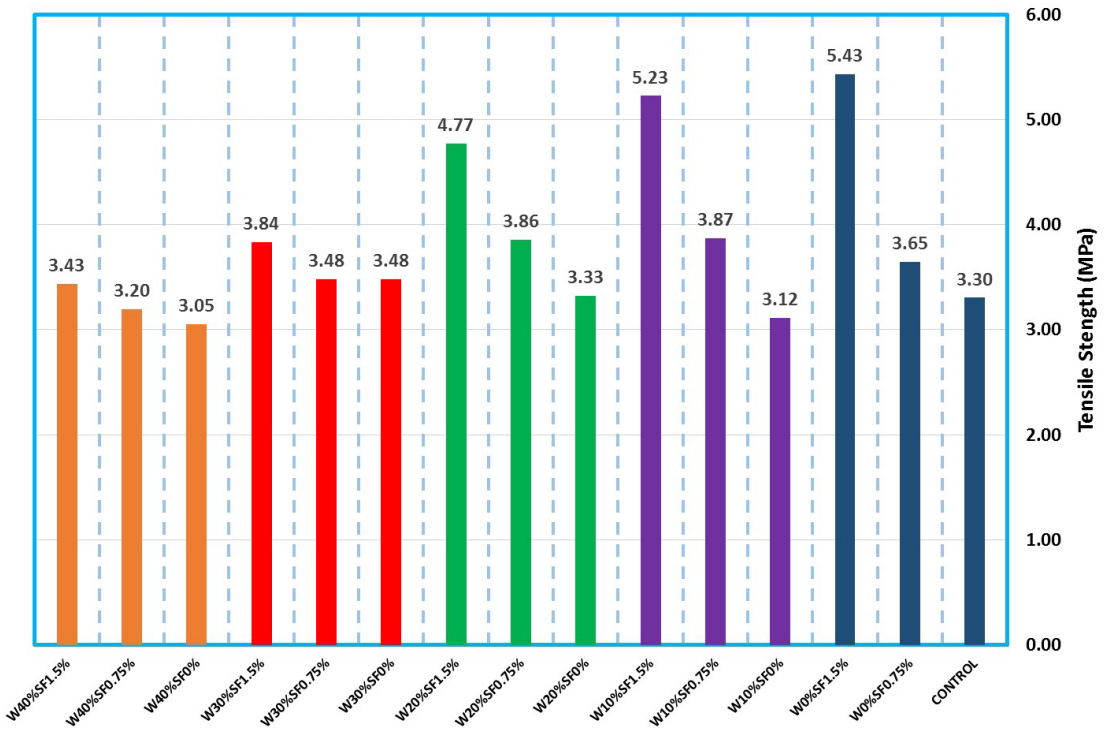

Figure 7. The tensile strength test results at 90 days curing ages.

The introduction of SFs significantly alters the tensile behavior across all replacement levels, as evidenced by the substantial increase in strength from 3.30 MPa to 3.65 MPa and 5.43 MPa at 0.75% and 1.5% fiber content in the 0% ceramic mixture; this enhancement is attributed to

the crack bridging action of the fibers, which restrain crack opening, delay crack propagation, and increase the composite's ability to sustain tensile stresses beyond the elastic limit. The effectiveness of SFs depends on the fiber–matrix bond, pull out resistance, and fiber dispersion, all of which are influenced by the microstructural characteristics of the matrix. In mixtures containing ceramic powder, the pozzolanic reaction enhances the ITZ by reducing portlandite crystals and filling voids with secondary C–S–H, thereby improving the mechanical anchorage of fibers and increasing their ability to transfer tensile stresses across developing cracks. This synergy is particularly evident in the 10% and 20% ceramic mixtures with 1.5% fiber content, which achieve tensile strengths of 5.23 MPa and 4.77 MPa, respectively—values that, while slightly lower than the 0% ceramic mixture with the same fiber dosage, still demonstrate strong fiber engagement and effective crack control. The slight reduction in tensile strength relative to the 0% ceramic mixture can be attributed to the reduced cement content and the transitional nature of the pozzolanic reaction at these replacement levels, which may not yet fully compensate for the loss of clinker. At 30% ceramic replacement, the tensile strength with 1.5% fiber content decreases further to 3.84 MPa, reflecting the diminishing ability of the matrix to mobilize fiber bridging capacity as the binder becomes increasingly reliant on pozzolanic activity; nevertheless, the presence of fibers still provides a significant improvement over the fiber free mixture, demonstrating that fiber reinforcement remains beneficial even when the matrix is weakened. At 40% replacement, the tensile strength with 1.5% fiber content drops to 3.43 MPa, confirming that excessive ceramic replacement compromises matrix integrity to the point where fiber anchorage is insufficient to sustain high tensile loads. From a microstructural perspective, the pozzolanic reaction contributes to matrix densification and ITZ strengthening, which enhances fiber–matrix interlock and improves the composite's resistance to crack initiation and propagation; this behavior aligns with established theories of ITZ enhancement in pozzolanic systems.

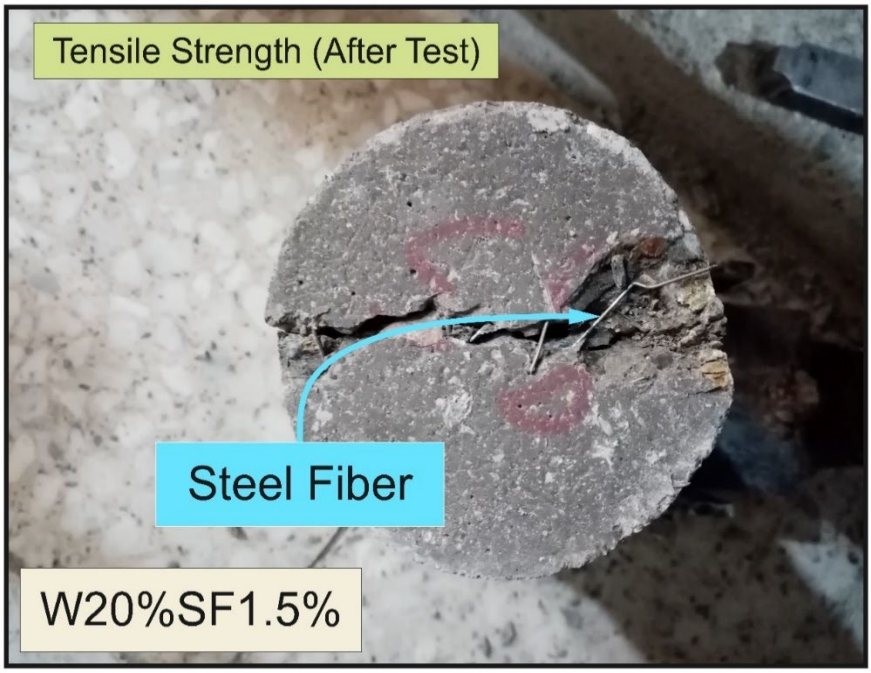

Figure 8. Post failure condition of the tensile specimen

The Brazilian test results also reveal that SFs transform the failure mode from brittle to quasi ductile, as fibers bridge the splitting crack, absorb energy through pull out and deformation, and provide residual tensile capacity even after matrix cracking. This ductility enhancement is consistent with the behavior expected from fiber reinforced composites designed for improved toughness and crack resistance. Overall, the results in Figure 7 demonstrate that WCP enhances long term tensile performance through pozzolanic activity, SFs significantly improve tensile strength through crack bridging mechanisms, and the combination of moderate ceramic replacement (10–20%) with 1.5% fiber content yields the most favorable balance between sustainability, microstructural refinement, and mechanical performance. These findings confirm the synergistic potential of integrating ceramic waste and SFs to produce high performance cementitious composites with superior tensile behavior at advanced curing ages.

The post failure condition of the Brazilian tensile specimen shown in Figure 8 provides a clear and instructive representation of the fracture mechanics governing fiber reinforced cementitious composites subjected to indirect tensile loading, revealing the critical role of SFs in controlling crack propagation, enhancing post peak resistance, and improving the overall toughness of the material. The cylindrical specimen, identified as mixture W20%SF1.5%, exhibits a well-defined diametral crack characteristic of the Brazilian splitting test, yet the presence of multiple SFs bridging the fracture plane demonstrates that the failure mode is not purely brittle; instead, it transitions into a quasi-ductile response due to the mechanical engagement of the fibers. As the applied compressive load induces tensile stresses perpendicular to the loading direction, microcracks initiate within the matrix and gradually coalesce into a dominant macrocrack along the diameter.

In a plain concrete specimen, this crack would propagate rapidly and uncontrollably, resulting in sudden catastrophic failure. However, in the fiber reinforced composite, the SFs embedded within the matrix act as bridging elements that transfer tensile stresses across the developing crack, delaying its propagation and significantly increasing the energy absorption capacity of the material. The exposed fibers visible in the fractured surface of the specimen confirm that many fibers underwent partial pull out rather than complete rupture, indicating a strong but not excessively rigid fiber–matrix bond, which is essential for achieving optimal toughness. The 20% waste ceramic powder used as a partial cement replacement contributes to this behavior by enhancing the microstructural quality of the matrix through its pozzolanic reaction, which consumes calcium hydroxide and forms additional C–S–H gel, thereby densifying the interfacial transition zone (ITZ) around the fibers. This improved ITZ increases the frictional resistance during fiber pull out, enabling the fibers to dissipate more energy as the crack widens. The combination of a refined matrix and well anchored fibers results in a composite capable of sustaining tensile stresses even after the matrix has cracked, which explains the elevated tensile strength observed in the experimental results. The crack pattern in Figure 8 also suggests that the fibers effectively controlled crack opening, as the fracture surfaces remain relatively aligned and the crack width is limited, demonstrating the fibers' ability to restrain crack widening under tensile stress. This behavior aligns with established fracture models for fiber reinforced concrete, where the post cracking response is governed by fiber pull out mechanisms rather than matrix cohesion. Overall, the specimen shown in Figure 8 validates the mechanical trends observed in the tensile strength results, confirming that the synergy between the pozzolanic ceramic powder and SFs enhances both the tensile capacity and the ductility of the composite, making it a promising material for applications requiring improved crack resistance and long-term durability.

3.4. Water Absorption

The 90-day water absorption results presented in Figure 9 provide a detailed understanding of how the combined effects of waste ceramic powder as a partial cement replacement and steel fiber reinforcement influence the permeability related behavior of the composite, revealing the complex interplay between matrix densification, pore structure refinement, and fiber–matrix interaction in determining the long-term durability performance of the material. The data clearly show that the incorporation of waste ceramic powder significantly reduces water absorption at moderate replacement levels, particularly when combined with SFs, demonstrating the beneficial role of the ceramic powder's pozzolanic reactivity, which enhances the microstructural integrity of the hardened matrix. In mixtures without SFs, water absorption decreases from 3.70% at 0% replacement to 3.09% at 10% and then slightly increases to 3.25% at 20%, rises further to 3.62% at 30%, and finally decreases again to 2.72% at 40%; this nonlinear trend reflects the balance between the beneficial effects of the pozzolanic reaction and the detrimental effects of excessive cement reduction. At 90 days, the amorphous aluminosilicate phases in the ceramic powder react with calcium hydroxide released during

cement hydration, forming additional C–S–H and C–A–S–H gels that fill capillary pores, reduce connectivity between voids, and strengthen the interfacial transition zone (ITZ).

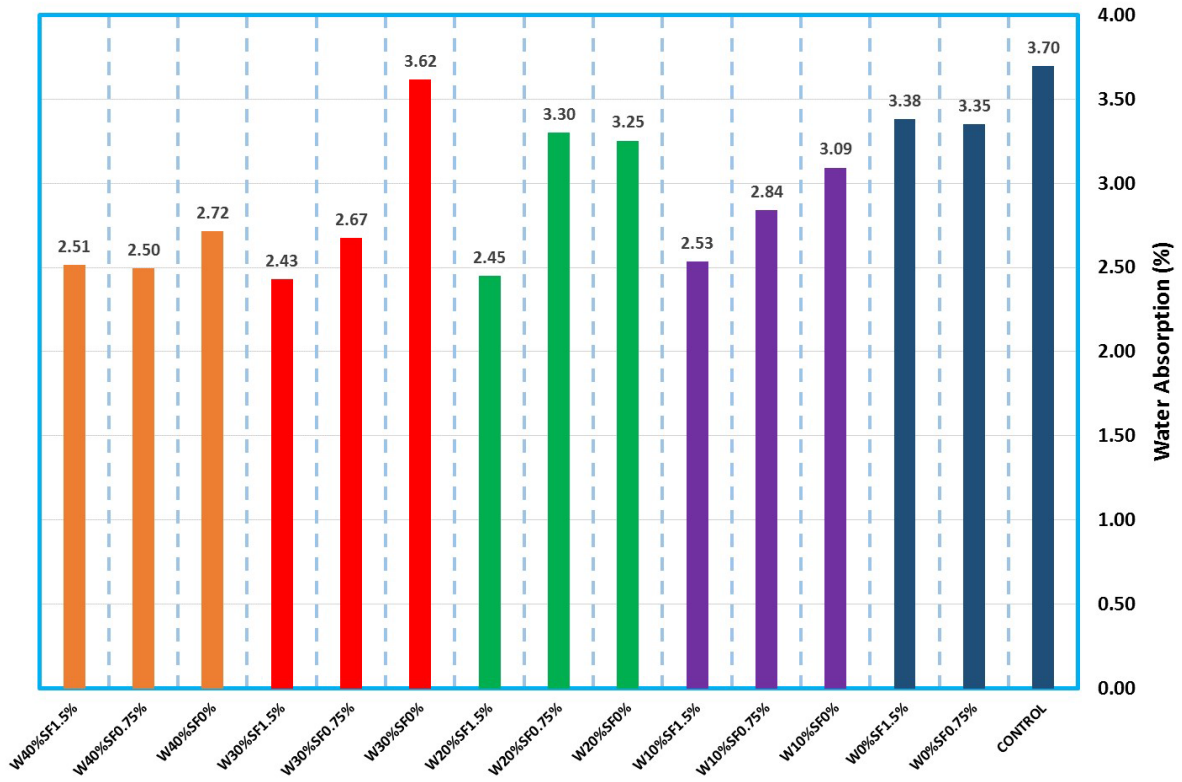

Figure 9. The water absorption test results at 90n days curing ages.

This microstructural refinement explains the significant reduction in water absorption at 10% replacement, where the pozzolanic reaction is sufficiently advanced to densify the matrix without compromising binder content. However, at 20% and 30% replacement, the water absorption increases due to the transitional nature of the pozzolanic reaction, which may not yet fully compensate for the reduction in clinker content, resulting in a matrix with partially refined but still interconnected pore networks. At 40% replacement, the water absorption decreases again, suggesting that the pozzolanic reaction becomes more dominant at later ages, producing enough secondary hydration products to offset the reduced cement content and refine the pore structure. The introduction of SFs significantly alters the water absorption behavior across all replacement levels, as evidenced by the consistent reduction in absorption values when fibers are added. For example, at 0% ceramic replacement, water absorption decreases from 3.70% to 3.35% and 3.38% with 0.75% and 1.5% fiber content, respectively, indicating that the presence of fibers reduces microcrack formation and limits pathways for water ingress. The beneficial effect of fibers becomes even more pronounced in mixtures containing ceramic powder: at 10% replacement, water absorption decreases from 3.09% to 2.84% and 2.53% with increasing fiber content; at 20% replacement, it decreases from 3.25% to 3.00% and 2.45%; and at 30% replacement, it decreases from 3.62% to 2.67% and 2.43%.

These results demonstrate a strong synergy between the pozzolanic matrix and the SFs, where the densified microstructure produced by the ceramic powder enhances the mechanical anchorage of fibers, while the fibers themselves limit crack formation and restrain crack widening, thereby reducing the permeability of the composite. The reduction in water absorption in fiber reinforced mixtures can be attributed to several mechanisms: (1) the fibers bridge microcracks that would otherwise serve as preferential pathways for water penetration, (2) the improved ITZ resulting from the pozzolanic reaction increases the frictional resistance during fiber pull out, reducing micro void formation around fibers, and (3) the combined effect of matrix densification and fiber reinforcement reduces the overall pore connectivity. The lowest water absorption values are observed in mixtures containing both ceramic powder and 1.5% steel fiber, particularly at 10%, 20%, and 30% replacement levels, where absorption values of 2.53%, 2.45%, and 2.43% indicate a highly refined and discontinuous pore structure. These results confirm that the integration of ceramic waste and SFs produces a composite with superior resistance to water ingress, which is a critical indicator of long-term durability, as lower water absorption is associated with reduced risk of chloride penetration, sulfate attack, freeze–thaw damage, and reinforcement corrosion. The behavior observed in Figure 9 therefore validates the synergistic interaction between the pozzolanic ceramic powder and SFs: the ceramic powder contributes to microstructural refinement and pore blocking through secondary hydration reactions, while the fibers enhance crack control and limit the formation of interconnected voids. Together, these mechanisms produce a composite with significantly improved durability characteristics, demonstrating that the combination of moderate ceramic replacement (10–30%) and steel fiber reinforcement is highly effective in reducing water absorption and enhancing the long-term performance of cementitious materials.

3.5. Life Cycle Assessment (LCA) with the Avoided Burden Approach

The environmental performance of the developed concrete mixtures was evaluated through a life cycle assessment (LCA) considering a functional unit of 1 m^3 of concrete. The system boundaries covered the main cradle-to-gate stages, including raw material extraction, aggregate production, transportation, processing of WCP, concrete mixing, and the incorporation of SFs. To properly capture the environmental benefit of using ceramic waste, the avoided burden approach was applied. Within this framework, the utilization of WCP provides a dual environmental advantage: it reduces the consumption of carbon-intensive Portland cement and simultaneously prevents the disposal of ceramic waste in landfills, thereby generating an environmental credit within the system boundary.

The life cycle inventory (LCI) was quantified using representative CO_2 emission factors commonly reported in concrete LCA databases. The adopted coefficients were 0.9 kg CO_2 per kg of Portland cement, 0.005 kg CO_2 per kg of natural aggregates, 1.7 kg CO_2 per kg of SFs, and 2 kg CO_2 per kg of superplasticizer. The environmental impact associated with the processing of WCP was estimated at 0.05 kg CO_2 per kg, while an environmental credit of 0.02

kg CO_2 per kg was assigned to represent the avoided impacts related to ceramic waste landfilling. These parameters formed the basis for the quantitative estimation of the carbon footprint of each concrete mixture.

In the reference mixture (W0%SF0%), the cement content was 400 kg/m³, which resulted in approximately 360 kg CO_2 emissions from cement production alone. The sand content (827 kg/m³) and coarse aggregates (1010 kg/m³) contributed 4.14 kg CO_2 and 5.05 kg CO_2, respectively. Additionally, the superplasticizer dosage (8 kg/m³) produced roughly 16 kg CO_2. By summing these contributions, the total carbon footprint of the control mixture was estimated at approximately 385 kg CO_2 per m³ of concrete.

The incorporation of SFs significantly increases the environmental burden due to the high energy intensity associated with steel production. In the mixture W0%SF0.75%, which contains 58.5 kg/m³ of SFs, an additional 99.5 kg CO_2 was generated, increasing the overall emissions to nearly 485 kg CO_2/m³. When the steel fiber dosage increased to 117 kg/m³ (W0%SF1.5%), the additional emissions reached approximately 199 kg CO_2, resulting in a total carbon footprint close to 585 kg CO_2/m³. These results indicate that although SFs enhance tensile and flexural performance, their use significantly increases embodied carbon when no cement replacement strategy is implemented.

For the concrete mixtures incorporating 10% WCP (W10%), the cement content decreased to 360 kg/m³, leading to a reduction in cement-related emissions to 324 kg CO_2. The processing of 40 kg of WCP generated approximately 2 kg CO_2, while the avoided landfill credit associated with ceramic waste corresponded to 0.8 kg CO_2. Consequently, the total emissions for the mixture W10%SF0% were estimated at about 350 kg CO_2/m³, representing roughly a 9% reduction compared with the control mixture. When SFs were introduced, the emissions increased to about 449 kg CO_2/m³ for W10%SF0.75% and 549 kg CO_2/m³ for W10%SF1.5%.

At a 20% replacement level (W20%), the cement consumption decreased further to 320 kg/m³, resulting in approximately 288 kg CO_2 emissions from cement production. The environmental burden associated with the processing of 80 kg of WCP was estimated at 4 kg CO_2, while the avoided waste disposal credit amounted to 1.6 kg CO_2. As a result, the total emissions for W20%SF0% were approximately 316 kg CO_2/m³. When SFs were incorporated, the total emissions increased to nearly 415 kg CO_2/m³ for W20%SF0.75% and 515 kg CO_2/m³ for W20%SF1.5%.

For the mixture containing 30% WCP (W30%), the cement content dropped to 280 kg/m³, producing approximately 252 kg CO_2 from cement manufacturing. The processing of 120 kg of WCP generated around 6 kg CO_2, while the avoided disposal of ceramic waste provided an environmental credit of –2.4 kg CO_2. Consequently, the total emissions for W30%SF0% were calculated to be approximately 280 kg CO_2/m³. With the addition of SFs, emissions increased to about 379 kg CO_2/m³ for W30%SF0.75% and 479 kg CO_2/m³ for W30%SF1.5%.

At the highest replacement level (40% WCP,), the cement content was reduced to 240 kg/m³, generating approximately 216 kg CO_2 from cement production. The processing of 160 kg of WCP contributed about 8 kg CO_2, while the avoided landfill credit amounted to –3.2 kg CO_2. Therefore, the total carbon footprint of the mixture W40%SF0% was estimated at around 244 kg CO_2/m³, which represents nearly a 37% reduction compared with the control mixture. With the addition of SFs, total emissions increased to approximately 343 kg CO_2/m³ for W40%SF0.75% and 443 kg CO_2/m³ for W40%SF1.5%.

When the environmental results are interpreted together with the mechanical performance data, an important trade-off becomes evident. Increasing the WCP replacement level significantly reduces CO_2 emissions due to the reduction in cement consumption; however, excessive replacement ratios above approximately 20–30% may lead to a decline in compressive strength. In contrast, the addition of SFs substantially improves tensile capacity and flexural strength—reaching values of approximately 6 MPa in certain mixtures which enhances crack resistance and structural ductility. From a performance-based LCA perspective, the mixtures W10%SF0.75% and W10%SF1.5% demonstrate a favorable balance between environmental and mechanical performance, maintaining compressive strengths in the range of 36–40 MPa while improving flexural behavior.

Overall, the results indicate that the substitution of Portland cement with WCP, when evaluated through the avoided burden methodology, can significantly reduce the embodied carbon of concrete production, achieving reductions of up to 37% compared with conventional concrete. Although the inclusion of SFs increases the embodied emissions due to the carbon intensity of steel manufacturing, their positive contribution to mechanical performance, crack control, and durability may extend the service life of concrete structures. Consequently, from a life-cycle perspective, the environmental cost associated with SFs can potentially be offset by reduced maintenance requirements and longer structural lifespan. Therefore, the optimal concrete mixture should be determined through a performance-based sustainability framework that simultaneously considers embodied carbon reduction, mechanical efficiency, and long-term durability to achieve truly sustainable concrete systems.

3.6. Pearson Correlation Analysis of Mechanical and Durability Parameters

The Pearson correlation matrix provides valuable insights into the statistical relationships between waste ceramic powder (WCP), steel fibers (SFs), and the mechanical and durability-related properties of concrete. Pearson correlation coefficients quantify the direction and magnitude of linear associations between variables; however, these relationships do not necessarily establish causality (Schober et al., 2018) [28]. The correlation matrix reveals strong negative correlations between WCP content and compressive strength at different curing ages, particularly at 90 days ($r = -0.87$) and 28 days ($r = -0.84$). These results indicate that increasing WCP replacement generally reduces compressive strength, primarily consistent with the cement dilution effect and the reduced availability of primary hydration products at higher

replacement levels. Similar observations were reported by Özkılıç et al. (2025), who demonstrated progressive deterioration in mechanical performance with increasing WCP content. Nevertheless, the moderate negative correlation between WCP and water absorption ($r = -0.56$) suggests that ceramic powder may contribute to pore refinement despite its adverse influence on compressive strength. This apparently contrasting behavior may arise from the competing effects of cement dilution, particle packing, and potential secondary pozzolanic reactions. Li et al. (2020) demonstrated that WCP can contribute to the formation of additional hydration products and microstructural refinement [26], while Ghonaim and Morsy (2023) reported reduced water absorption at moderate ceramic waste replacement levels [15]. Accordingly, the observed correlation trends may be associated with improved matrix compactness and refinement of the interfacial transition zone (ITZ), although these mechanisms require direct microstructural verification.

In contrast, SF content exhibits strong positive correlations with splitting tensile strength ($r = 0.72$) and flexural strength ($r = 0.75$), highlighting the dominant contribution of fibers to tensile-controlled mechanical behavior. These relationships are consistent with the findings of Song and Hwang (2004), who attributed the enhanced tensile and flexural performance of steel fiber-reinforced concrete to crack bridging, stress redistribution, and resistance to crack propagation. Furthermore, the moderate negative correlation between SF content and water absorption ($r = -0.58$) suggests that fiber reinforcement may contribute to restricting microcrack development and limiting pathways for water ingress. Nevertheless, the effectiveness of this mechanism depends on fiber dosage, dispersion, fiber–matrix bonding, and matrix compactness. Conversely, the weak-to-moderate negative correlations between SF content and compressive strength ($r = -0.30$ to -0.43) indicate that increasing fiber dosage does not necessarily improve compressive performance. This behavior may be associated with reduced workability, entrapped air, and localized disturbances in matrix compactness, particularly at higher fiber volume fractions. Comparable observations were reported by Alegre Cornelio et al. (2024), who demonstrated that the combined incorporation of ceramic powder and SFs improved tensile and flexural strengths without necessarily enhancing compressive strength [27].

The correlation matrix also reveals a very strong positive association between 14-day and 28-day compressive strengths ($r = 0.93$), reflecting consistent age-dependent strength development across the investigated mixtures. Similarly, the strong positive correlation between splitting tensile and flexural strengths ($r = 0.89$) suggests that both properties are influenced by common mechanical mechanisms, particularly fiber-mediated stress transfer and crack-bridging capacity. Collectively, these statistical relationships demonstrate the complementary roles of WCP and SFs: WCP primarily influences matrix composition, compressive strength, and water absorption, whereas SFs predominantly govern tensile and flexural performance. Nevertheless, their combined contribution depends on the balance between binder dilution, potential microstructural refinement, and mechanical reinforcement.

Integrating the correlation analysis with the experimental results, particularly the water absorption trends presented in Figure 10, indicates that moderate WCP replacement levels of 10–20% provide a favorable compromise between mechanical performance, resistance to water ingress, and reduced Portland cement consumption. Although the 10% replacement level generally provides superior compressive performance, the 20% replacement level offers lower water absorption, suggesting potential improvements in pore structure and matrix compactness. These observations are consistent with previous investigations emphasizing the importance of optimizing ceramic waste replacement levels rather than maximizing cement substitution (Li et al., 2020; Ghonaim and Morsy, 2023; Özkılıç et al., 2025) [19, 26, 27]. When combined with 1.5% SFs, the composite benefits from enhanced tensile and flexural resistance through fiber-bridging mechanisms, while maintaining satisfactory compressive performance and reduced water absorption.

From a multi-response perspective, identifying a favorable concrete composition requires simultaneous consideration of competing mechanical, durability-related, and sustainability objectives, rather than maximizing an individual performance indicator (Hurtado-Alonso et al., 2025) [29]. Accordingly, among the investigated mixtures, the composition containing 20% WCP and 1.5% SFs can be identified as a favorable balanced formulation based on the combined experimental evidence and observed statistical relationships. This composition offers enhanced tensile and flexural performance, reduced water absorption, and satisfactory compressive strength while reducing Portland cement consumption by 20%. Nevertheless, formal multi-objective optimization and additional durability and microstructural investigations are recommended to establish its optimality and long-term performance under different environmental exposure conditions.

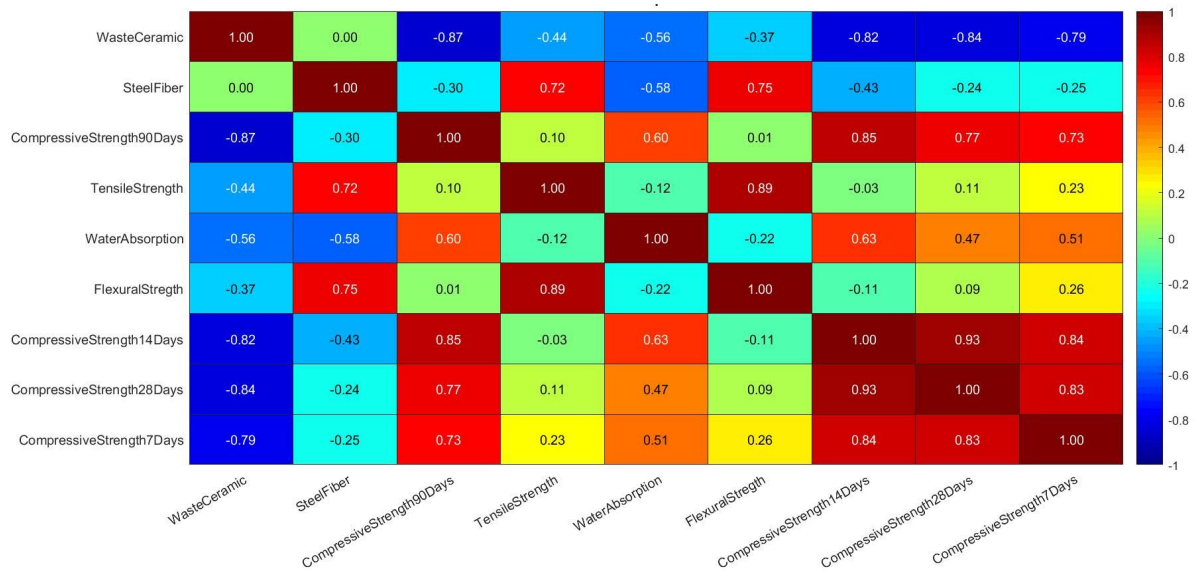

Figure 10. Pearson correlation matrix illustrating the statistical relationships among mechanical and durability parameters.

3.7. Cubic Regression-Based Surface Response Modeling of Mechanical and Durability Properties

Figures 11 and 12 present the output of the cubic regression modeling as 3D surface plots, accurately illustrating the synergistic interaction between the WCP replacement percentage and the Steel Fiber (SF) volume fraction on the mechanical and durability properties of the concrete. The determined regression coefficients along with the corresponding R^2 values for each fitted surface are summarized in Table 3. In Figure 11, the compressive strength development at 7, 14, 28, and 90 days is analyzed; the complex curvature of the surfaces highlights the non-linear nature of these variables, where the addition of SF consistently enhances strength, while the effect of WCP varies depending on the replacement level and curing age. During early hydration stages (7 and 14 days), high replacement levels of WCP slightly suppress early strength gains due to cement dilution, whereas prolonged curing up to 90 days facilitates the secondary pozzolanic reaction, densifying the interfacial transition zone (ITZ) and substantially recovering strength. The high coefficient of determination (R^2) values, ranging from 0.8984 to 0.9903 as reported in Table 3, demonstrate the model's high precision in fitting the experimental data (shown as red points) and its capability to predict hydration kinetics and the filler effects of WCP over time.

Table 3. Numerical coefficients (p_0 to p_9) and for the third-order (cubic) response surface models predicting concrete mechanical and durability properties

	Tensile Strength	Compressive Strength (90 Days)	Water Absorption %	Flexural Strength	Compressive Strength (14 Days)	Compressive Strength (28 Days)	Compressive Strength (7 Days)
p0	3.1686	39.7480	3.5600	2.5698	38.5016	39.6286	27.0811
p1	0.0241	0.1735	-0.0694	0.0366	0.0884	-0.1725	0.5835
p2	0.9668	-46.9961	-7.0826	5.1309	-28.4700	16.1512	11.9538
p3	-0.0008	-0.0244	0.0048	0.0025	-0.0298	-0.0167	-0.0327
p4	-0.9503	94.3105	13.9285	-3.9284	45.7788	-39.2416	-22.7283
p5	0.0106	-0.2136	-0.0526	-0.1325	0.1402	0.1872	-0.3664
p6	0.0000	0.0004	-0.0001	-0.0001	0.0005	0.0003	0.0004
p7	0.8814	-42.3962	-6.1991	1.5294	-21.0114	16.5289	9.6187
p8	-0.0002	0.0043	0.0011	0.0006	-0.0035	-0.0074	0.0038
p9	-0.0262	0.0355	0.0042	0.0363	0.1007	0.1543	0.1342

Figure 12 displays the surface plots for splitting tensile strength, flexural strength, and water absorption at 90 days. It is observed that tensile and flexural strengths show a strong positive correlation with increasing fiber dosage, which is predominantly governed by the crack-bridging mechanism of the steel fibers across microcracks, thereby enhancing post-cracking load transfer and energy absorption. Conversely, the water absorption surface exhibits a more complex, oscillatory behavior, reflecting the intricate interplay between concrete porosity,

cementitious replacement materials, and fiber dispersion; moderate additions of fine ceramic powder optimize particle packing and lower permeable porosity, whereas excessive inclusions paired with high fiber contents marginally promote void formation through fiber clustering. Unlike simple linear models, the adoption of a third-degree regression in this analysis has allowed for the precise identification of optimal points and regions of maximum mechanical performance. The proximity of experimental data to the fitted surfaces and the high R^2 values (e.g., 0.9732 for tensile strength and 0.9488 for flexural strength) confirm that the derived empirical models in Table 3 provide a reliable predictive tool for optimizing concrete mix designs containing waste ceramics and SFs, thereby reducing the need for costly and time-consuming repetitive testing.

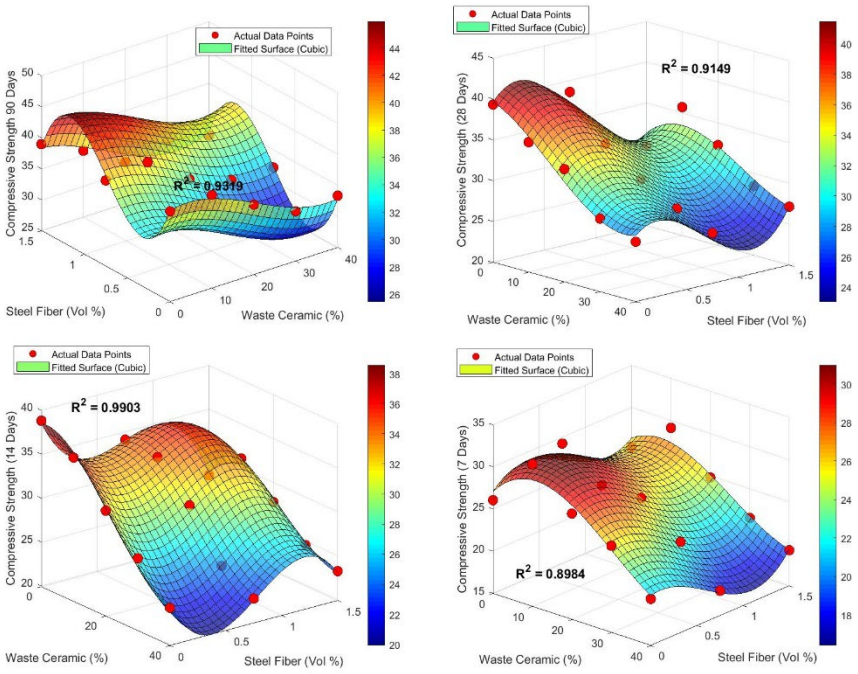

Figure 11. Cubic regression modeling as 3D surface plots (Compressive Strength)

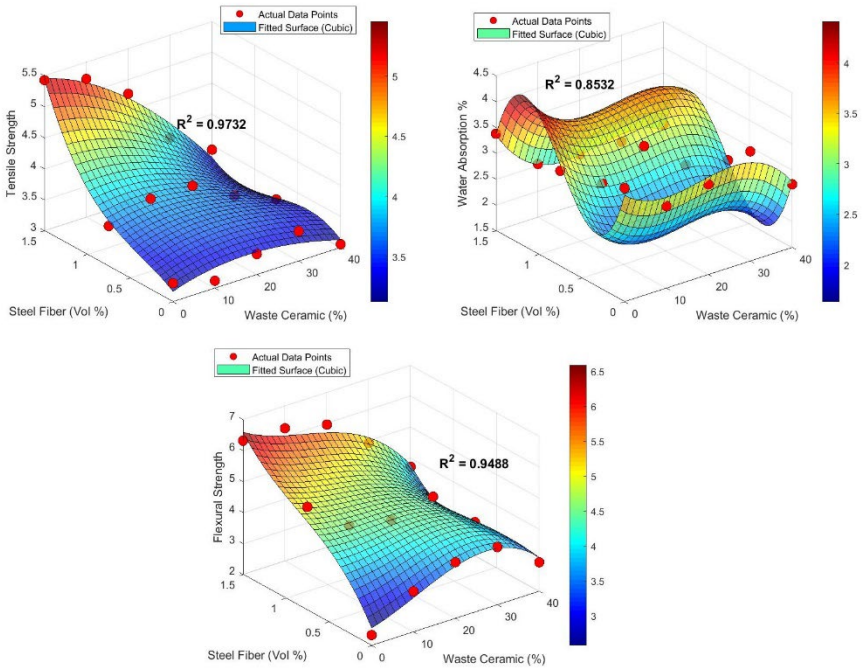

Figure 12. Cubic regression modeling as 3D surface plots (Flexural and Tensile Strength, Water Absorption)

4. Conclusion

This study demonstrated the successful incorporation of WCP and SFs (SFs) in concrete as a sustainable approach to improve both environmental performance and mechanical properties. The experimental results showed that partial replacement of cement with WCP can enhance concrete behavior at moderate levels, particularly around 10% replacement, where compressive strength reached its optimum value. However, higher replacement ratios generally caused strength reduction due to the dilution of cementitious materials. The addition of SFs significantly improved flexural behavior and crack resistance through an effective crack-bridging mechanism, while their influence on compressive strength was limited. The combined use of WCP and SFs produced a synergistic effect, where WCP contributed to matrix densification through filler and pozzolanic reactions, and SFs enhanced toughness, ductility, and post-cracking performance. Among the investigated mixtures, the best overall performance was observed at moderate WCP contents combined with fiber reinforcement, especially in mixtures containing 10–20% WCP and 0.75–1.5% SFs. Furthermore, the statistical regression analysis confirmed strong correlations between the mixture parameters and the measured responses, indicating that the proposed models can reliably predict concrete performance. Overall, the findings confirm that WCP and SFs can be effectively used to develop eco-friendly, high-performance concrete with reduced cement consumption, improved mechanical characteristics, and lower environmental impact, supporting sustainable construction and circular economy objectives.

5. References

AlArab, A., Hamad, B., Chehab, G., & Assaad, J. (2020). Use of ceramic-waste powder as value-added pozzolanic material with improved thermal properties. *Journal of Materials in Civil Engineering, 32*(9), 04020243. https://doi.org/10.1061/(ASCE)MT.1943-5533.0003275

American Society for Testing and Materials. (2021). *Standard test method for compressive strength of cylindrical concrete specimens* (ASTM C39/C39M-21). https://doi.org/10.1520/C0039_C0039M-21

American Society for Testing and Materials. (2023). *Standard specification for concrete aggregates* (ASTM C33/C33M-18). https://doi.org/10.1520/C0033_C0033M-18

Behbahani, H., Nematollahi, B., & Farasatpour, M. (2011). Steel fiber reinforced concrete: A review. In *Proceedings of the International Conference on Structural Engineering, Construction and Management (ICSECM2011)*.

Behforouz, B., Tavakoli, D., & Haratian, M. (2020). Regression and ANN models for durability and mechanical characteristics of waste ceramic powder high performance sustainable concrete. *Computers & Concrete, 25*(2), 119–132. https://doi.org/10.12989/cac.2020.25.2.119

Bhargava, A., & Banthia, N. (2008). Permeability of concrete with fiber reinforcement and service life predictions. *Materials and Structures, 41*(2), 363–372. https://doi.org/10.1617/s11527-007-9246-9

Cornelio, M. K. A., Huayllas, K. J. S., & Pasapera, K. L. L. (2024). Influence of partial replacement of cement by ceramic powder and addition of steel fibers on the mechanical properties of concrete. *Proceedings of the LACCEI International Multi-Conference for Engineering, Education, and Technology, 1*(10). https://doi.org/10.18687/LACCEI2024.1.1.788

Gaffke, N., & Heiligers, B. (1996). Approximate designs for polynomial regression: Invariance, admissibility, and optimality. In S. Ghosh & C. R. Rao (Eds.), *Handbook of statistics* (Vol. 13, pp. 1149–1199). Elsevier. https://doi.org/10.1016/S0169-7161(96)13026-2

Gautam, L., Kalla, P., & Jethoo, A. S. (2021). A review on the utilization of ceramic waste in sustainable construction products. *Materials Today: Proceedings, 43*, 1884–1891. https://doi.org/10.1016/j.matpr.2020.09.756

Ghonaim, S., & Morsy, R. (2023). Utilization of ceramic waste material as cement substitution in concrete. *Buildings, 13*(8), 2067. https://doi.org/10.3390/buildings13082067

Heidari, A., & Tavakoli, D. (2013). A study of the mechanical properties of ground ceramic powder concrete incorporating nano-SiO2 particles. *Construction and Building Materials, 38*, 255–264. https://doi.org/10.1016/j.conbuildmat.2012.07.041

Hurtado-Alonso, N., et al. (2024). Optimization of cementitious mixes through response surface method: A systematic review. *Archives of Civil and Mechanical Engineering, 25*(1), 54. https://doi.org/10.1007/s43452-024-01112-3

Kannan, D. M., Aboubakr, S. H., El-Dieb, A. S., & Reda Taha, M. M. (2017). High performance concrete incorporating ceramic waste powder as large partial replacement of Portland cement. *Construction and Building Materials, 144*, 35–41. https://doi.org/10.1016/j.conbuildmat.2017.03.018

Korat, A., Amin, M., & Tahwia, A. M. (2025). A comprehensive assessment of ceramic wastes in ultra-high-performance concrete. *Innovative Infrastructure Solutions, 10*(1), 28. https://doi.org/10.1007/s41062-024-01806-w

Li, L., Liu, W., You, Q., Chen, M., & Zeng, Q. (2020). Waste ceramic powder as a pozzolanic supplementary filler of cement for developing sustainable building materials. *Journal of Cleaner Production, 259*, 120853. https://doi.org/10.1016/j.jclepro.2020.120853

Li, L., Huang, Z., Tan, Y., & Kwan, A. K. H. (2024). A study of some relevant properties of concrete incorporating waste ceramic powder as a cement replacement agent. *Journal of Building Engineering, 87*, 109106. https://doi.org/10.1016/j.jobe.2024.109106

Lopez, V., Llamas, B., Juan, A., Morán, J. M., & Guerra, I. (2007). Eco-efficient concretes: Impact of the use of white ceramic powder on the mechanical properties of concrete. *Biosystems Engineering, 96*(4), 559–564. https://doi.org/10.1016/j.biosystemseng.2006.12.004

Mahasenan, N., Smith, S., & Humphreys, K. (2003). The cement industry and global climate change: Current and potential future cement industry CO2 emissions. In J. Gale & Y. Kaya (Eds.), *Greenhouse gas control technologies—6th international conference* (pp. 995–1000). Pergamon. https://doi.org/10.1016/B978-008044276-1/50157-4

Mohit, M., & Sharifi, Y. (2019). Thermal and microstructure properties of cement mortar containing ceramic waste powder as alternative cementitious materials. *Construction and Building Materials, 223*, 643–656. https://doi.org/10.1016/j.conbuildmat.2019.07.009

Nasr, D., Babagoli, R., & Dehaghani, A. K. (2025). Enhancing sustainable concrete using waste ceramic powder and natural pozzolan through experimental and machine learning approaches. *Scientific Reports, 15*(1), 44198. https://doi.org/10.1038/s41598-025-27964-0

Özkılıç, Y. O., Aksoylu, C., Arslan, M. H., & Güneş, A. (2025). Waste ceramic powder for sustainable concrete production as supplementary cementitious material. *Frontiers in Materials, 11*, 1450824. https://doi.org/10.3389/fmats.2024.1450824

Pacheco-Torgal, F., & Jalali, S. (2010). Reusing ceramic wastes in concrete. *Construction and Building Materials, 24*(5), 832–838. https://doi.org/10.1016/j.conbuildmat.2009.10.023

Schober, P., Boer, C., & Schwarte, L. A. (2018). Correlation coefficients: Appropriate use and interpretation. *Anesthesia & Analgesia, 126*(5), 1763–1768. https://doi.org/10.1213/ANE.0000000000002864

Song, P., & Hwang, S. (2004). Mechanical properties of high-strength steel fiber-reinforced concrete. *Construction and Building Materials, 18*(9), 669–673. https://doi.org/10.1016/j.conbuildmat.2004.04.027

Subaşı, S., Öztürk, H., & Emiroğlu, M. (2017). Utilizing of waste ceramic powders as filler material in self-consolidating concrete. *Construction and Building Materials, 149*, 567–574. https://doi.org/10.1016/j.conbuildmat.2017.05.013

Taher, M. J., Abed, E. H., & Hashim, M. S. (2023). Using ceramic waste tile powder as a sustainable and eco-friendly partial cement replacement in concrete production. *Materials Today: Proceedings*. https://doi.org/10.1016/j.matpr.2023.04.060

Tang, K. (2025). Assessing stray DC and AC current-induced corrosion in steel fiber-reinforced concrete (SFRC) in railway tunnelling construction. *International Journal of Civil Engineering, 23*(1), 43–55. https://doi.org/10.1007/s40999-024-01018-4

Tawfik, T. A., El-Aziz, M. A., Abd El-Aziz, M., & Faried, A. S. (2024). Sustainable reuse of waste ceramic tiles powder and waste brick powder as a replacement for cement on green high strength concrete properties. *Innovative Infrastructure Solutions, 9*(5), 166. https://doi.org/10.1007/s41062-024-01498-2

Thomas, J., & Ramaswamy, A. (2007). Mechanical properties of steel fiber-reinforced concrete. *Journal of Materials in Civil Engineering, 19*(5), 385–392. https://doi.org/10.1061/(ASCE)0899-1561(2007)19:5(385)